Experimental Observation of a Time-Driven Phase Transition in Quantum Chaos

Clément Hainaut,[1] Ping Fang,[2,3] Adam Rançon,[1] Jean-François Clément,[1] Pascal Szriftgiser,[1] Jean-Claude Garreau,[1] Chushun Tian,[3,1,*] and Radu Chicireanu[1,3,†]

[1]*Université de Lille, CNRS, UMR 8523—PhLAM—Laboratoire de Physique des Lasers Atomes et Molécules, F-59000 Lille, France*[‡]

[2]*Institute for Advanced Study, Tsinghua University, Beijing 100084, China*

[3]*CAS Key Laboratory of Frontiers in Theoretical Physics and Institute of Theoretical Physics, Chinese Academy of Sciences, Beijing 100190, China*

(Received 25 February 2018; published 27 September 2018; corrected 29 January 2019)

We report the first experimental observation of the time-driven phase transition in a canonical quantum chaotic system, the quantum kicked rotor. The transition bears a firm analogy to a thermodynamic phase transition, with the time mimicking the temperature and the quantum expectation of the rotor's kinetic energy mimicking the free energy. The transition signals a sudden change in the system's memory behavior: before the critical time, the system undergoes chaotic motion in phase space and its memory of initial states is erased in the course of time; after the critical time, quantum interference enhances the probability for a chaotic trajectory to return to the initial state, and thus the system's memory is recovered.

DOI: 10.1103/PhysRevLett.121.134101

Quantum chaos is usually defined as the behavior of a quantum system whose classical limit is chaotic [1], and has long been an elusive subject. Quantum and classical chaos may differ dramatically because Schrödinger's equation is linear, and does not lead to the sensitivity to initial conditions, which is the main characteristic of classical chaos. A particularly important consequence is that classical chaos erases the memory of initial states rapidly, whereas quantum chaos can remember an initial state at long times. A natural question is thus, how, precisely, the interplay between classical chaos and quantum effects leads to the recovery of memory. For sufficiently short times, the behavior of a quantum system is (largely) *classical*; only after quantum interference effects are built up has the dynamics become truly quantum. For quantum chaos this happens at the so-called Ehrenfest time, when quantum-classical correspondence breaks down [2]. This question is crucial not only to understand quantum-classical correspondence in chaotic systems but also to realize quantum control of chaos. In addition, it can shed new light on many intriguing chaotic phenomena found in a variety of quantum systems recently (see, e.g., Refs. [3–9]). Whereas this interplay has been investigated theoretically from different perspectives [10–17], experimental results are rare: most experiments focus on the deep quantum regime, where information on classical chaos is difficult to extract, and thus cannot address the interplay and memory recovering processes.

The experimental results and the theoretical interpretation presented in this work show the existence of a time-driven phase transition directly related to this interplay. By studying the early dynamics of a quantum chaotic system, we observe a nonanalyticity in the time dependence of a measurable observable. This nonanalyticity is a direct evidence of a sudden change in the system's memory behavior, which can be attributed to the subtle quantum interference effects arising from the *quantum chaotic* nature of the system. This is a striking difference between the classical chaotic and the quantum chaotic behaviors, shedding important new light on classical to quantum chaos transition.

We study a "standard model" of quantum chaos, the quantum kicked rotor (QKR), which is a quantum particle moving on a ring under the influence of sequential pulsed driving in time ("kick") [18]. Despite its simplicity, the QKR embodies the most important properties of generic quantum chaotic systems, the realization of which remains challenging. As such, the QKR has become a paradigmatic system in experimental studies of quantum chaos (see Ref. [19] for a review). Its Hamiltonian is time dependent and assumes a general form,

$$\hat{H}(t) = \frac{\hat{p}^2}{2} + K\cos[\hat{x} - a(t)]\sum_n \delta(t-n), \qquad (1)$$

where all quantities are rescaled and dimensionless (see below the description of the experiment for details). The first term in $\hat{H}(t)$ describes the rotor's free motion and the second the driving switched on at integer times $t = n$, the kicking strength is K, and the reduced Planck's constant $\bar{k}$ gives $[\hat{x}, \hat{p}] = i\bar{k}$. The above model differs from the standard QKR by the presence of a phase modulation $a(t)$. By varying $a(t)$, rich dynamical phenomena arise. When $a(t)$ is constant, the system reduces to the standard

QKR, which exhibits dynamical localization, an analog of Anderson localization in one-dimensional disordered systems [20]. When $a(t)$ is modulated by $(d-1)$ incommensurate frequencies which are all, as well as $\hbar$, incommensurate with 2π, the system is equivalent to a d-dimensional periodic QKR and can simulate the Anderson transition in d dimensions [21,22]. When $a(t+N)=a(t)$ $(N=2,3,\ldots)$, the *periodically shifted* QKR results, whose studies were initiated in Ref. [16] and have been advanced recently [23,24]. Below we will focus on the standard and the periodically shifted QKR.

The QKR allows us, for the first time, to study experimentally the memory recovery in quantum chaotic systems. The basic idea is as follows. First, the rotor's memory behavior can be characterized by the time correlation function of angular position, defined as [10]

$$C_q(t) \equiv \frac{K^2}{2}\langle 0|\sin\hat{x}(t)\sin\hat{x}(0)+\sin\hat{x}(0)\sin\hat{x}(t)|0\rangle, \quad (2)$$

where $|p\rangle$ stands for the unperturbed angular momentum state. Then, as shown in Supplemental Material [25], C_q has a simple relation to the expectation value of the rotor's energy growth, $\frac{1}{2}\langle\delta p^2(t)\rangle \equiv \frac{1}{2}\langle p^2(t)-p^2(0)\rangle$, which is

$$C_q(t) = \frac{1}{2}\frac{d^2}{dt^2}\langle\delta p^2(t)\rangle. \quad (3)$$

This suggests that the rotor's memory behaviors can be probed by the time derivatives of $\langle\delta p^2(t)\rangle$. Crucially, as $\langle\delta p^2(t)\rangle$ can be measured directly in experiments, we can explore how the system's memory behaviors change in time.

Building on this idea, we performed an experiment on the atom-optics realization of QKR, and measure the energy growth $\langle\delta p^2(t)\rangle$ at early time; see below for details. We found that $\langle\delta p^2(t)\rangle$ displays a nonanalyticity at some critical time t_E^*. More precisely, the second-order derivative of $\langle\delta p^2(t)\rangle$ has a discontinuity:

$$C_q(t) = \begin{cases} 0 & t < t_E^* \\ c(t-t_E^*)^{-\nu} & t > t_E^*, \end{cases} \quad (4)$$

where a positive (vanishing) exponent ν corresponds to the divergence (jump), and the lower order derivatives are continuous. The value of ν is completely determined by the system's symmetry, and is universal with respect to the system's details. The latter only affect the values of t_E^* and the proportionality coefficient c. Loosely speaking, t_E^* marks the onset of quantum interference and thus has the same physical meaning as the Ehrenfest time. The Ehrenfest time is a very difficult quantity to access experimentally, and our work reports its first measurement. Equation (4) shows, quantitatively, that the system's memory behavior undergoes a *sudden change*: for $t < t_E^*$, the memory of the initial states is erased, while from t_E^* on quantum interference starts destroying classically chaotic behavior and the memory is recovered.

From Eqs. (3) and (4) we see that the nonanalyticity of $C_q(t)$ bears a firm analogy to the second-order phase transitions in thermodynamics. To be specific, t mimics the temperature, $\langle\delta p^2(t)\rangle$ the free energy, and ν the critical exponent. This behavior arises from the interplay between classical chaos and quantum interference, and is thus expected to hold in more general quantum chaotic systems. Note that time-driven phase transitions in quantum systems have attracted much attention recently, both theoretically and experimentally [26–28], but so far investigations have been restricted to nonchaotic systems. Our results give new insight on the fundamental aspects of dynamical phase transitions, from the perspective of quantum chaotic systems.

In order to discuss a physical picture for phenomena discussed above, we first show how changing the periodic modulation of $a(t)$ leads to distinct symmetries. Let us start from the simplest case, $N=1$, namely, the standard QKR. The transformation $t\to -t$, $\hat{x}\to -\hat{x}$, $\hat{p}\to\hat{p}$ leaves $\hat{H}(t)$ invariant. Thus, the standard QKR bears time-reversal (T_c) symmetry, with $\hat{x}$ mimicking the electron momentum and $\hat{p}$ the position in conventional disordered electronic systems [29]. Owing to this symmetry, the dynamical localization in the standard QKR [18,20] is an analog of Anderson localization in time-reversal invariant spinless systems [30]. For $N>2$, other symmetry classes can be realized [16,24]. In particular, one can randomly choose the modulation configuration: $\{a(0)=0, a(1),\ldots,a(N-1)\}$. In this case, the Floquet operator is a product of N successive one-step evolution operators, and can be checked to break the T_c symmetry [31]. The ensuing dynamical localization is an analog of Anderson localization in broken time-reversal systems [16]. The symmetry effects of periodic modulation can manifest in distinct fluctuation behaviors of the quasieigenenergy spectrum of Floquet operators [25].

The origin of the observed time-driven phase transition can be understood from simple arguments, and a heuristic determination of the "critical exponent" ν can be obtained for distinct symmetries. The Wigner representation yields a natural connection between classical and quantum rotors. In this representation a quantum state corresponds to a Planck's cell of size $\hbar$ in the phase space, spanned by the coordinates x and p; in the classical limit $\hbar\to 0$, the cell shrinks to a point and a classical state results. For short evolution times, $t < t_E^*$, quantum effects basically play no role, and the center of Planck's cell moves along a classical trajectory. As the classic dynamics is chaotic, trajectories initially close to each other separate exponentially at later times. Hence, the memory of the initial state $\gamma_0 \equiv (x(0), p(0))$ is erased; i.e., γ_0 is uncorrelated with the evolving state $\gamma_t \equiv (x(t), p(t))$, and $C_q(t)$ defined by Eq. (2) vanishes [Fig. 1(i)]. For long evolution times,

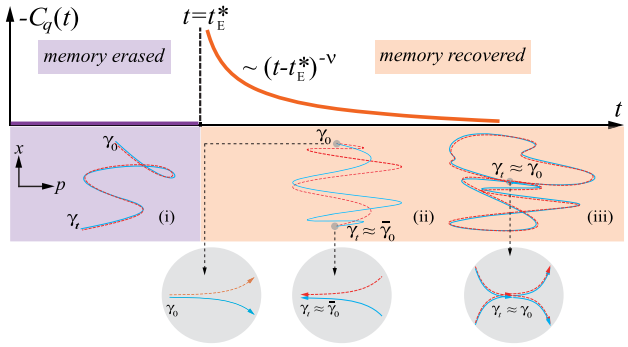

FIG. 1. The time-driven phase transition at the critical time t_E^* (top) signals a sudden change in system's memory behavior (middle). For $t < t_E^*$, the system wanders randomly in phase space, and the initial state γ_0 and the evolving state γ_t are uncorrelated (i). For $t > t_E^*$, two trajectories (blue solid and red dashed lines) departing from Planck's cell centered at γ_0, due to dynamical instability (bottom), can interfere constructively and meet again with a significant probability in the same cell (iii) or in the cell (ii) centered at $\bar{\gamma}_0$ (which is the time-reversed conjugate of γ_0) after long wandering; thus the memory of the initial state is recovered.

$t > t_E^*$, due to dynamical instability, trajectories initiating from the same Planck's cell reach a large separation at t_E^* (Fig. 1, bottom left) and wander independently at later times. However, interferences between trajectories can enhance the probability for them to meet again in the initial cell centered at γ_0 (Fig. 1, bottom right) or its time-reversal conjugate, centered at $\bar{\gamma}_0 \equiv (-x(0), p(0))$ (Fig. 1, bottom middle), depending on whether the T_c symmetry is absent or present. The memory of the initial state is thereby recovered. We consider separetely two cases.

(i) *T_c-symmetric case.*—A trajectory connecting γ_0 and $\bar{\gamma}_0$ and its time reversal have the same phase [Fig. 1(ii)] and thus interfere constructively. Therefore, the probability for them to meet in the cell centered at $\bar{\gamma}_0$ is enhanced. Since the motion in the p direction is diffusive, the probability is $\sim (t - t_E^*)^{-1/2}$. This gives the critical exponent:

$$\nu = 1/2. \tag{5}$$

In addition, when the trajectory returns to the origin of momenta [$p(t) = p(0)$], one has $x(t) = -x(0)$ (recall that x mimics the electron velocity in usual disordered systems). This interference effect is called, in the context of disordered systems, *coherent backscattering*. Moreover, because $x(t) = -x(0)$, we find $C_q(t) \sim \sin x(t) \sin x(0) < 0$.

(ii) *Broken T_c symmetry case.*—A trajectory can pass the cell centered at γ_0 twice, forming two loops in phase space [Fig. 1(iii)]. A trajectory passing these two loops has the same phase as the one passing the same loops in the reversed order, they thus interfere constructively with each other even in the absence of T_c symmetry; the probability of returning simultaneously to the initial cell γ_0 is thus enhanced. This probability can be estimated as $\sim \int_{t_E^*}^{t} dt'/\sqrt{(t'-t_E^*)(t-t')} = \pi(t-t_E^*)^0$, with each inverse square root factor accounting for the probability of forming a loop. Thus, the critical exponent is

$$\nu = 0. \tag{6}$$

Because the trajectory returns to the origin of momenta with $x(t) = x(0)$, this effect is called *coherent forward scattering* [32]. In addition, because $x(t) = x(0)$, the corresponding contribution to $C_q(t)$ is $\sim \sin x(t) \sin x(0) > 0$. In fact, there is another contribution which is of the same order but negative, arising from the *backward scattering* $x(t) = -x(0)$. It dominates the positive contribution [cf. Eq. (9) below]; thus, $C_q(t) < 0$.

Having summarized the findings and discussed their physical implications, we now present a detailed description of the experiment and its theoretical analysis. We used an atomic kicked rotor realization [33] with laser-cooled atoms. Cesium atoms of mass M are submitted to a periodic series (of period T_1) of pulses of a one-dimensional sinusoidal potential, of a short duration τ. The potential is realized using a far-detuned laser standing wave (SW), formed by two independent counterpropagating laser beams, with wave number k_L. If the distance traveled by the atom during the pulse duration τ is small compared to k_L^{-1}, the pulse can be considered as a Dirac function, and the atom's motion is described by the Hamiltonian Eq. (1), where time is rescaled by T_1, space by $1/(2k_L)$, and momentum by $M/(2k_L T_1)$. In these units, the reduced Planck's constant is $\bar{k} = 4\hbar k_L^2 T_1/M$ ($\hbar$ is the Planck's constant). The scaled kick amplitude is $K \propto I/|\Delta|$, with I the maximum laser intensity and Δ the laser-atom detuning. The phase shift $a(t)$ in Eq. (1) is realized by imposing a relative phase between the two laser beams forming the standing wave, whose temporal profile can be easily changed [24].

We load a cloud of about 10^6 cesium atoms in a standard magneto-optical trap and cool it to a temperature of a few microkelvin by an optimized molasses. The cloud is then exposed to pulses of a vertical SW with the following parameters: wavelength 852 nm, $T_1 = 9.6$ μs, $\tau = 0.2$ μs, $\Delta = -13$ GHz (spontaneous emission can thus be neglected during the experiments), waist 0.8 mm, and $I = 30$ W/cm^2. By adding a linear chirp of the relative frequency of the beams, we generate a SW whose nodes are accelerated, and this acceleration is adjusted to match the gravity's acceleration, so that in the (noninertial) reference frame in which the SW is at rest, an inertial force exactly compensates gravity [22]. At the end of the kick sequence, the atomic momentum distribution $\Pi(p, t)$ is detected by a standard time-of-flight measurement. From $\Pi(p, t)$ we obtain [34]

$$\delta\langle p^2(t)\rangle = \int dp p^2 [\Pi(p, t) - \Pi(p, 0)]. \tag{7}$$

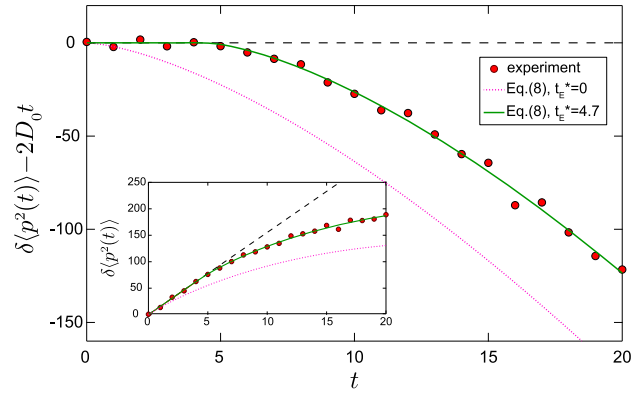

FIG. 2. Experiments on the standard QKR ($N = 1$, $K = 5.5$, $\bar{k} = 1$), that displays T_c symmetry, confirm a time-driven phase transition, manifesting in the time profile of $\delta\langle p^2(t)\rangle - 2D_0 t$. Experimental data (symbols) are well described by Eq. (8), with $t_{\rm loc}$ and t_E^* treated as fitting parameters, and show a time singularity at $t_E^* = 4.7$ (green solid line). The data are incompatible with $t_E^* = 0$ (pink dotted line). Inset: Same as main panel, showing $\delta\langle p^2(t)\rangle$ instead. The black dashed line represents the linear growth due to diffusion.

In order to explore the interplay between quantum effects and classical chaos, a small $\bar{k}$ is preferable, so that the timescale at which localization effects dominate is longer than the duration of the experiment [18,20]. However, the requirement that $\tau \ll T_1$ prevents us from reaching too small values $\bar{k}$ [36]; we thus choose $\bar{k} \simeq 1$ in the experiments.

We first consider the standard QKR [i.e., $a(t+N) = a(t)$ with $N = 1$], which exhibits the T_c symmetry. The decoherence rate that limits the duration of the experiments increases with K, so we choose $K = 5.5$, for which the classical dynamics is strongly chaotic [37]. The measurements of $\delta\langle p^2(t)\rangle$ are displayed in the inset of Fig. 2. At early times, its growth is linear, $\delta\langle p^2(t)\rangle = 2D_0 t$ with D_0 the diffusion coefficient, corresponding to the classical chaotic behavior. This implies that the system wanders stochastically in phase space and exhibits a (normal) diffusion in momentum. Figure 2, displaying $\delta\langle p^2(t)\rangle - 2D_0 t$, clearly shows that the growth is purely linear up to a critical time t_E^*, from which it starts to deviate from the classical behavior.

To determine t_E^* and analyze the measurements beyond this critical time, we need to turn the qualitative discussions above on the origin of the time singularity into a quantitative theory. This has been done by one of us and coworkers in Refs. [15,16] by using the diagrammatic technique, leading to the Ehrenfest time-dependent weak dynamical localization theory. According to that theory, for the standard QKR we have

$$\delta\langle p^2(t)\rangle = 2D_0\left(t - \frac{4}{3\sqrt{\pi}}\theta(t - t_E^*)\frac{(t - t_E^*)^{3/2}}{t_{\rm loc}^{1/2}}\right), \quad (8)$$

where $t_{\rm loc}$ is the localization time and $\theta(t)$ the Heaviside function. The scaling law $\sim(t - t_E^*)^{3/2}$ accounts for the weak dynamical localization, arising from constructive interference between a trajectory and its time reversal [Fig. 1(ii)], which exists only for $t \geq t_E^*$. Equation (8) shows that $\delta\langle p^2(t)\rangle$ measured at integer t can be embedded into a curve which is continuous in t. This curve exhibits a singularity at the Ehrenfest time t_E^* (not necessarily an integer). Namely, upon taking the second-order derivative of Eq. (8) we obtain Eq. (4), and the exponent $\nu = 1/2$, as expected from the qualitative discussions (Fig. 1). Numerical simulations confirming this behavior at small $\bar{k}$ (not achievable experimentally) are presented in the Supplemental Material [25].

Equation (8) was derived analytically for $K \gg 1 \gg \bar{k}$. For present parameters we expect it to remain valid qualitatively—as the physical picture of the second term is quite general—but not quantitatively. We will thus use $t_{\rm loc}$ as an additional fitting parameter. Our fitting procedure of the experimental data is as follows: First, we pick a time t_0, and perform a *linear* fit $\delta\langle p^2(t)\rangle$ from $t = 0$ to $t = t_0$ to extract a diffusion coefficient D_0; we then perform a two-parameter fit of the full data using t_E^* and $t_{\rm loc}$ as parameters (keeping D_0 fixed); if $t_0 > t_E^*$ or if $t_0 \ll t_E^*$, we reestimate D_0 by setting t_0 to t_E^* and repeat the procedure until t_0 and t_E^* converge. As shown in Fig. 2, the measurements are in good agreement with Eq. (8) for $t_{\rm loc} = 33$ and $t_E^* = 4.7$. A vanishing t_E^*, as predicted in the QKR analog [38] of standard weak localization in disordered systems [39], is clearly inconsistent with the experimental data.

The weak dynamical localization theory with broken T_c symmetry [16] can be generalized to the periodically shifted QKR. Specifically, we have

$$\delta\langle p^2(t)\rangle = 2D_0\left(t + \sum_{i=1}^{2}\frac{(-1)^i}{it_{\rm loc}}\theta(t - t_{Ei}^*)(t - t_{Ei}^*)^2\right), \quad (9)$$

where the last two terms are weak dynamical localization corrections, and the Ehrenfest times $t_{E1,2}^*$ are different in general. Comparing Eqs. (8) and (9), we find that the power 3/2 law is replaced by a quadratic law. This is because when the T_c symmetry is broken, the constructive interferences between two trajectories have more complicated patterns. In particular, the term with $i = 2$ in Eq. (9) is positive, corresponding to the pattern shown in Fig. 1(iii). The positivity arises from the forward scattering: $x(t) = x(0)$ when a trajectory returns to the momentum origin; i.e., $p(t) = p(0)$. The second term is negative, and the negativity arises from the backward scattering: $x(t) = -x(0)$ when $p(t) = p(0)$.

To experimentally realize a periodically shifted QKR with broken T_c symmetry, we set $N = 4$, $\bar{k} = 1$, and $K = 3.9$, and average over 100 sets $\{a(1), a(2), a(3), a(4)\}$ picked randomly [31]. We have checked numerically that the classical dynamics is strongly chaotic. Figure 3 displays the measurements of $\delta\langle p^2(t)\rangle$, and we use the same fitting procedure as above to extract first D_0 and then $t_{\rm loc}$, t_{E1}^*, and t_{E2}^*. Good

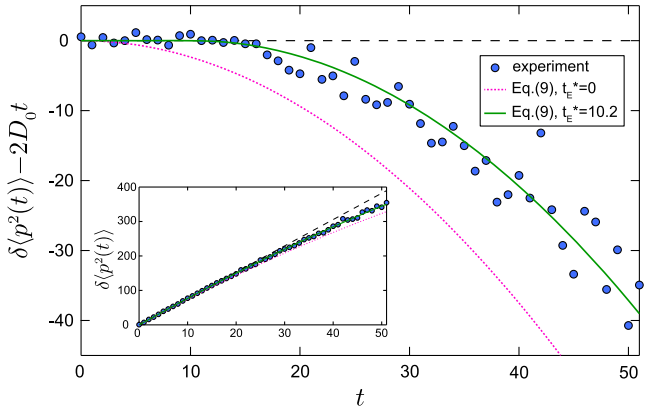

FIG. 3. Experiments measuring $\delta\langle p^2(t)\rangle - 2D_0 t$ with the periodically shifted QKR with broken T_c symmetry ($N = 4$, $K = 3.9$, $\bar{k} = 1$). Experimental data (circles) are well described by Eq. (9), with $t_{\rm loc}$ and t_E^* treated as fitting parameters, and show a time singularity at $t_E^* = 10.2$ (green full line). The data are incompatible with $t_E^* = 0$ (pink dotted line). Inset: Same as main panel, showing $\delta\langle p^2(t)\rangle$ instead. The black dashed line represents the linear growth corresponding to diffusion.

agreement with measurements is found if we set $t_{E1}^* = t_{E2}^* (\equiv t_E^*)$, which yields $t_E^* = 10.2$ and $t_{\rm loc} = 163$. These data do not, however, allow us to clearly distinguish different $t_{E1,2}^*$ values, because of the limited accessible parameter range. We also see that when $t_{E1,2}^*$ are set to zero, Eq. (9) is incompatible with the measurements. This provides strong evidence of a time singularity at finite t_E^*, with $\nu = 0$, which again signals a sudden change in the system's memory behavior.

In conclusion, our measurements are fully compatible with the existence of a time-driven phase transition in quantum chaotic systems, with the critical time being the Ehrenfest time. We took advantage of the flexibility of ultracold atoms experiments to finely study exotic effects in the short-time dynamics of quantum chaotic systems. This paves the way for a detailed study of the all-time dynamics of such systems. Finally, we remark that the QKR is a one-body system. In the future, it would be interesting to theoretically investigate the time-driven phase transition in many-body quantum chaos currently under intensive investigations [4,40].

We thank V. Galitski, J. Wang, and L. W. Zhou for useful discussions. This work is supported by Agence Nationale de la Recherche (Grant K-BEC No. ANR-13-BS04-0001-01), the Labex CEMPI (Grant No. ANR-11-LABX-0007-01), the Ministry of Higher Education and Research, Hauts de France Council and European Regional Development Fund (ERDF) through the Contrat de Projets Etat-Region (CPER Photonics for Society, P4S), and the National Natural Science Foundation of China (Grants No. 11535011 and No. 11747601).

C. H. and P. F. contributed equally to this work.

*ct@itp.ac.cn
†rchicireanu@gmail.com
‡www.phlam.univ-lille1.fr/atfr/cq

[1] F. Haake, *Quantum Signatures of Chaos*, 2nd ed. (Springer-Verlag, Berlin, 2001).
[2] A. I. Larkin and Y. N. Ovchinnikov, Sov. J. Exp. Theor. Phys. **28**, 1200 (1969).
[3] P. Hayden and J. Preskill, J. High Energy Phys. 09 (2007) 120.
[4] J. Maldacena and D. Stanford, Phys. Rev. D **94**, 106002 (2016).
[5] J. Maldacena, S. H. Shenker, and D. Stanford, J. High Energy Phys. 08 (2016) 106.
[6] A. A. Patel and S. Sachdev, Proc. Natl. Acad. Sci. U.S.A. **114**, 1844 (2017).
[7] I. L. Aleiner, L. Faolo, and L. B. Ioffe, Ann. Phys. (Amsterdam) **375**, 378 (2016).
[8] Y. Chen and C. Tian, Phys. Rev. Lett. **113**, 216802 (2014).
[9] C. Tian, Y. Chen, and J. Wang, Phys. Rev. B **93**, 075403 (2016).
[10] D. L. Shepelyansky, Physica (Amsterdam) **28D**, 103 (1987).
[11] G. Casati and B. V. Chirikov, *Quantum Chaos: Between Order and Disorder* (Cambridge University Press, Cambridge, England, 1995).
[12] I. L. Aleiner and A. I. Larkin, Phys. Rev. B **54**, 14423 (1996).
[13] V. V. Sokolov and O. V. Zhirov, Eur. Phys. Lett. **84**, 30001 (2008).
[14] G. Benenti and G. Casati, Phys. Rev. E **79**, 025201(R) (2009).
[15] C. Tian, A. Kamenev, and A. Larkin, Phys. Rev. Lett. **93**, 124101 (2004).
[16] C. Tian, A. Kamenev, and A. Larkin, Phys. Rev. B **72**, 045108 (2005).
[17] E. B. Rozenbaum, S. Ganeshan, and V. Galitski, Phys. Rev. Lett. **118**, 086801 (2017).
[18] G. Casati, B. V. Chirikov, J. Ford, and F. M. Izrailev, Lect. Notes Phys. **93**, 334 (1979).
[19] J. C. Garreau, C. R. Phys. **18**, 31 (2017).
[20] S. Fishman, D. R. Grempel, and R. E. Prange, Phys. Rev. Lett. **49**, 509 (1982).
[21] G. Casati, I. Guarneri, and D. L. Shepelyansky, Phys. Rev. Lett. **62**, 345 (1989).
[22] I. Manai, J.-F. Clément, R. Chicireanu, C. Hainaut, J. C. Garreau, P. Szriftgiser, and D. Delande, Phys. Rev. Lett. **115**, 240603 (2015).
[23] C. Hainaut, I. Manai, R. Chicireanu, J.-F. Clément, S. Zemmouri, J. C. Garreau, P. Szriftgiser, G. Lemarié, N. Cherroret, and D. Delande, Phys. Rev. Lett. **118**, 184101 (2017).
[24] C. Hainaut, I. Manai, J.-F. Clément, J. C. Garreau, P. Szriftgiser, G. Lemarié, N. Cherroret, D. Delande, and R. Chicireanu, Nat. Commun. **9**, 1382 (2018).
[25] See Supplemental Material at http://link.aps.org/supplemental/10.1103/PhysRevLett.121.134101 for additional technical details of the analytical theory.
[26] M. Heyl, A. Polkovnikov, and S. Kehrein, Phys. Rev. Lett. **110**, 135704 (2013).

[27] P. Jurcevic, H. Shen, P. Hauke, C. Maier, T. Brydges, C. Hempel, B. P. Lanyon, M. Heyl, R. Blatt, and C. F. Roos, Phys. Rev. Lett. **119**, 080501 (2017).
[28] M. Heyl, Rep. Prog. Phys. **81**, 054001 (2018).
[29] K. Efetov, *Supersymmetry in Disorder and Chaos* (Cambridge University Press, Cambridge, England, 1997).
[30] C. Tian and A. Altland, New J. Phys. **12**, 043043 (2010).
[31] In principle, antisymmetric sequences should be excluded (see Supplemental Material [25]), but the probability of randomly picking one of them is negligible.
[32] T. Karpiuk, N. Cherroret, K. L. Lee, B. Grémaud, C. A. Müller, and C. Miniatura, Phys. Rev. Lett. **109**, 190601 (2012).
[33] F. L. Moore, J. C. Robinson, C. F. Bharucha, B. Sundaram, and M. G. Raizen, Phys. Rev. Lett. **75**, 4598 (1995).
[34] In order to determine $\delta\langle p^2(t)\rangle$, we use a two-component test function [35] to fit the shape of measured $p^2\Pi(p,t)$. We verified that this procedure agrees very well with results of numerical simulations.
[35] O. I. Lobkis and R. L. Weaver, Phys. Rev. E **71**, 011112 (2005).
[36] To consider the kicks as Dirac functions, the distance traveled by the atoms during the kicks should be much smaller than the wavelength of the standing wave. This enforces $\tau \sim 200$ ns for the present experimental setup. On the other hand, the condition $\tau \ll T_1$ must be met also. Putting these two constraints together, we require $\bar{k} \geq 1$.
[37] B. V. Chirikov, Phys. Rep. **52**, 263 (1979).
[38] A. Altland, Phys. Rev. Lett. **71**, 69 (1993).
[39] L. P. Gor'kov, A. I. Larkin, and D. E. Khmel'nitskii, J. Exp. Theor. Phys. Lett. **30**, 228 (1979).
[40] S. Sachdev and J. Ye, Phys. Rev. Lett. **70**, 3339 (1993).

Correction: The previously published Figs. 2 and 3 contained errors in the curve keys and the caption to Fig. 3 referred to the wrong equation. These errors have been fixed.